Determining bathymetry of shallow and ephemeral desert lakes using satellite imagery and altimetry

Moshe Armon[1,1], Elad Dente[2,2], Yuval Shmilovitz[1,1], Amit Mushkin[3,3], Tim J Cohen[4,4], Efrat Morin[2,2], and Yehouda Enzel[1,1]

[1]Hebrew University of Jerusalem
[2]Institute of Earth Sciences, The Hebrew University of Jerusalem
[3]Geological Survey of Israel
[4]University of Wollongong

November 30, 2022

Abstract

Water volume estimates of shallow desert lakes are the basis for water balance calculations, important both for water resource management and paleohydrology/climatology. Water volumes are typically inferred from bathymetry mapping; however, being shallow, ephemeral and remote, bathymetric surveys are scarce in such lakes. We propose a new, remote-sensing based, method to derive the bathymetry of such lakes using the relation between water occurrence, during >30-yr of optical satellite data, and accurate elevation measurements from the new Ice, Cloud, and Land Elevation Satellite-2 (ICESat-2). We demonstrate our method at three locations where we map bathymetries with ˜0.3 m error. This method complements other remotely sensed, bathymetry-mapping methods as it can be applied to: (a) complex lake systems with sub-basins, (b) remote lakes with no in-situ records, and (c) flooded lakes. The proposed method can be easily implemented in other shallow lakes as it builds on publically accessible global data sets.

Determining bathymetry of shallow and ephemeral desert lakes using satellite imagery and altimetry

M. Armon[1], E. Dente[1,2,3], Y. Shmilovitz[1,2], A. Mushkin[2], T. J. Cohen[4], E. Morin[1], and Y. Enzel[1]

[1]The Fredy and Nadine Herrmann Institute of Earth Sciences, the Hebrew University of Jerusalem, Israel.

[2]The Geological Survey of Israel, Israel.

[3]Shamir Research Institute, University of Haifa, Israel.

[4]School of Earth and Environmental Sciences, University of Wollongong, Australia.

Corresponding author: Moshe Armon (moshe.armon@mail.huji.ac.il)

Key Points:

- A new methodology to produce bathymetry maps of shallow desert lakes was developed, based on globally available datasets
- The methodology enables mapping the bathymetry of lakes with sub-basins or partially flooded lakes; both major limitations of other methods
- The derived bathymetry error is ~30 cm, rather than ~2.5 m for other globally available data

Abstract

Water volume estimates of shallow desert lakes are the basis for water balance calculations, important both for water resource management and paleohydrology/climatology. Water volumes are typically inferred from bathymetry mapping; however, being shallow, ephemeral and remote, bathymetric surveys are scarce in such lakes. We propose a new, remote-sensing based, method to derive the bathymetry of such lakes using the relation between water occurrence, during >30-yr of optical satellite data, and accurate elevation measurements from the new Ice, Cloud, and Land Elevation Satellite-2 (ICESat-2). We demonstrate our method at three locations where we map bathymetries with ~0.3 m error. This method complements other remotely sensed, bathymetry-mapping methods as it can be applied to: (a) complex lake systems with sub-basins, (b) remote lakes with no in-situ records, and (c) flooded lakes. The proposed method can be easily implemented in other shallow lakes as it builds on publically accessible global data sets.

Plain Language Summary

Lakes in desert environments are often remote, shallow, and only get filled once in a long while. They are an important water resource, and could be used to decipher past environmental conditions. However, detailed maps of lake-floor terrain, which are required to effectively study these lakes are typically not available. The deepest parts of the lakes are filled with water more frequently than their shallow margins. Thus, we suggest here to relate water occurrence in those lakes with accurate satellite-based elevation measurements, to obtain a valuable lake-floor terrain map. We demonstrate the usefulness of our method by comparing results with other globally available data. Previous methods struggle with complex-terrain lakes or lakes that are partially flooded during their survey; while our method yields high-resolution accurate maps even in such lakes.

1 Introduction

A major characteristic of drylands is endoreism, internal drainage (de Martonne, 1927). The lower and usually drier parts of these drylands are often occupied by ephemeral or seasonal shallow desert lakes (Nicholson, 2011). Thousands of such lakes exist globally with the largest being Lake Eyre (Australia, alias Kati Thanda; surface area of >9000 km^2 when full). Such lakes are significant for opportunistic species that have no other water resources (e.g., D'Odorico and Porporato, 2006; Noy-Meir, 1973). Mapping of lake floors is key in calculating water balance (e.g., Cohen et al., 2015; Enzel and Wells, 1997), important in water resources management, and in deciphering paleoehydrology (e.g., Crétaux et al., 2016; Quade et al., 2018). However, being shallow, dry and remote, bathymetric surveys (e.g., as in Bye et al., 1978) have been scarce in such lakes.

A different approach to bathymetry mapping is through remote-sensing (Gao, 2015; Jawak et al., 2015). The Shuttle Radar Topography Mission (SRTM) has provided high resolution (~30m) global digital elevation models (DEMs) that could, in principal, present bathymetry of such desert lakes. Yet, radar altimetry cannot produce accurate DEMs if the area is flooded or where lake floors are exceptionally bright and/or smooth (Berry et al., 2007; Brenner et al., 2007), which are common conditions.

To improve lake-bathymetry maps, recent studies either integrate remote-sensing data with a spatial interpolation of in-situ measurements (Feng et al., 2011; Leon and Cohen, 2012) or combine between optical imaging and radar (e.g., Sun and Ma, 2019) or laser altimetry (Arsen et al., 2013; Li et al., 2019; Ma et al., 2019). These satellite imaging methods are based on determining isobaths (equal depth lines) of a lake, through snapshots during different lake stages. Then, shorelines in each specific image are assigned a height through accurate elevation measurements; such as laser altimetry. This determines bathymetry only to the depth of the lowest shoreline identified, using a spatial interpolation of a few isobaths. It also overlooks the possible variance in elevation of a specific shoreline, which can be significant in large lakes (Arsen et al., 2013; Feng et al., 2011). Li et al. (2019) suggested using a long-term (410 images during >30-yr) water occurrence index, instead of a few specific isobaths, and relating it with measurements from a limited dataset of airborne lidar altimetry. This overcomes shoreline elevation variations and

makes spatial interpolation unnecessary. However, they assumed a linear relation between isobath areas, sampled at specific points, and elevation. Applying their methodology to a deep reservoir (Lake Mead; >100m deep) only revealed the bathymetry of the upper part of the lake; the deeper bathymetry was extrapolated with geometrical considerations, calibrated using in-situ data (Li et al., 2019). A further complication arises where water occurrence is not based directly on elevation, primarily where a lake is composed of a few sub-basins, which yields more than one possible relation between water occurrence and elevation. Accordingly, present-day methodologies and freely available datasets cannot provide accurate, high-resolution bathymetry of often-flooded, shallow desert lakes, especially for lakes having more than one sub-basin.

Thus, to derive the bathymetry of desert lakes, there is a need for: (a) an efficient and reliable way to recognize the water occurrence at a high resolution, (b) a technique to overcome diverse water occurrences-elevation relations in different sub-basins, (c) a way to derive the bathymetry when lakes are inundated, and (d) a robust method to validate the resultant bathymetry. To tackle these challenges, we developed a simple and easily implemented methodology that derives bathymetry of shallow desert lakes. This paper focuses on three desert lakes, ranging in area from 0.2×10^3 km^2 to 6×10^3 km^2. Lake bathymetries are acquired using the relation between globally-available high-resolution (30 m) water occurrence maps, and elevation data from NASA's new Ice, Cloud, and Land Elevation Satellite-2 (ICESat-2).

Following is a description of the methodology and its application over Lake Eyre, which consists of a few sub-basins. We show the derivation of a bathymetric map for the lake and validate it versus the global SRTM and the best bathymetric map available for the region (Section 3). Having better results than the SRTM, we set to derive the bathymetry of a remote lake in the Sahara (Sabkhat El-Mellah) that has no other bathymetric map (Section 4) and of Lago Coipasa in the Altiplano for which we separately derive the bathymetry under dry and inundated conditions.

2 Methodology

Desert lakes are often fed by floods with monthly to decadal frequencies. Most of the coarser particles are deposited upstream, and thus, lake floors are mainly covered with fine low-permeability sediments, making evaporation the primary output (Nicholson, 2011). Water occurrence in these lakes is <100% of the time, and often <30%. Thanks to a detailed analysis of 3×10^6 Landsat images by Pekel et al. (2016), the frequency of water occurrence over 30 m pixels between 1984 and 2015 is easily accessible worldwide. Water occurs more often over the deeper parts of the lake, where complete evaporation takes longer, and less often over the higher lake margins. Thus, there should be a straightforward relation between water occurrences (i.e., the relative frequency of water in a pixel) and lake floor elevation over such lakes. This, in turn, allows measuring height over specific locations within the lake, from which we can infer the entire lake floor elevation.

ICESat-2 provides dense and accurate elevation measurements (0.7 m point spacing; accuracy and precision of <5 cm and <13 cm, respectively) over land, and even underwater. Thus it yields accurate, narrow (~14m) height profiles of Earth surface, since its launch in September 2018, with a 91-day revisiting frequency (Brunt et al., 2019; Markus et al., 2017). Underwater measurements can penetrate up to ~1 Secchi depth (Parrish et al., 2019), i.e. up to a few meters or even a few dozens of meters (Ma et al., 2019), depending on the optical properties of the water.

To derive bathymetry maps we rely on the relation between Water Occurrence and Laser Profile elevation (hereon WOLP) using four (to five) steps (described schematically in the supporting information Figure 1 [S1]): (a) acquiring a lake water occurrence map from the global water occurrence (Pekel et al., 2016); (b) extracting ICESat-2 elevation data (ATL03 product) that coincide with the lake (defined as regions with >0% water occurrence) (Figure 1a); (c) fitting a mathematical function describing the relation between water occurrence values and elevations (Figure 1b) based on all available scans in the lake extent; and (d) applying the fitted function areally, to translate the water occurrence map into lake-floor elevation over the entire lake basin (Figure 1d). For lakes consisting of sub-basins, an additional step is needed between steps c and d, in which we identify lake sub-basins from water occurrence, as detailed in Section 3 (e.g., Figure 1c). This methodology provides a bathymetric map of lakes that were flooded to some extent between 1984 and 2015, with a resolution of ~30 m.

To evaluate our methodology, we use available topographic data to demonstrate differences between our results and available bathymetric (or topographic) maps. Where the SRTM is the best external source, we use cross-validation, putting aside one ICESat-2 scan each time and validating the bathymetry based on all other scans. Owing to the high accuracy of the ICESat-2 data, we demonstrate the small expected error using our methodology.

3 Lake Eyre

Lake Eyre (Figure 2c, e) has a watershed covering almost 1% of the global land area (>1.1×10^6 km^2). It has a complex lake floor with a minimum elevation of -15.2 m relative to the Australian Height Datum (AHD) (Kotwicki and Isdale, 1991). The great flood of 1974 was utilized to perform bathymetric surveys over the lake, yielding a 0.5-m-contour-interval bathymetric map and detailing features >1 km^2 (Bye et al., 1978). Leon & Cohen (2012) (hereon LC12) combined data from this bathymetric map with SRTM data and ICESat-1 laser altimetry (with 170 m point spacing) to form the best bathymetric map of the lake that we are aware of. Because of its vast size, complex bathymetry, and a good reference map, we chose to apply our methodology over Lake Eyre. To have a continuous map, we only mapped Lake Eyre North (the larger and more frequently flooded part of the lake).
To overcome complexity arising from the different relations of water occurrence and elevation in each of the sub-basins (Figure 1b), we divided Lake Eyre North into five sub-basins using the water occurrence map (Figure 1a, S2). This enabled identification of pseudo watersheds, similar to determining watersheds in a topographic map (Supporting Information 1 [SI1]; Schwanghart and Scherler (2014)). We then performed steps b to d of our methodology, separately for each sub-basin (as exampled in Figure 1c). If more than one ICESat-2 scan intersected a watershed, we used data from all available scans. To form a single map out of the different sub-basins, regions close to the pseudo water divide were assigned values using step c from all neighboring sub-basins, inversely weighted according to their distance from the divide (SI1).

We validated the WOLP bathymetry map (Figure 1d) against SRTM data and the LC12 bathymetry over the entire region (Table 1, Figures 2a, 2b), and against ICESat-2 scans over the measured profiles (Figure S3). The WOLP bathymetry lies within ±0.5 m of LC12 elevations for 74% of the region (90% is within ±1 m), i.e., it lies within one elevation contour of Bye et al. (1978). Most of the remaining areas (deviating >1 m) are situated next to the lake margins, where the LC12 map is mostly based on SRTM data, which were acquired during a lake inundation interval, and are therefore not reliable over major parts of the lake (Leon and Cohen, 2012). In ~83% of the area SRTM data were replaced by a constant elevation value (-15 m AHD). The root mean square difference (RMSD) of the SRTM data versus the LC12 map is 1.77 m, and only 25% of the SRTM data are within ±0.5 m of LC12, whereas the WOLP bathymetry has a RMSD of 0.52 m (Table 1). Moreover, the mean RMSD for each of the sub-basins using cross-validation of the different ICESat-2 scans is 0.21-0.57 m (Figure S4), indicating that the WOLP map error is even smaller than it seems when comparing it to the LC12 map.
Hypsometric curves emphasize differences between these analyzed bathymetries (Figure 3), and are important for water volume estimates (SI2). Whereas the SRTM wet area sharply increases above the minimum elevation, because of the constant (-15 m) elevation polygon, the WOLP and the LC12 wet area curves present a gradual increase with depth (Figure 3a). Accordingly, water volumes are lower by ~75% both in the WOLP and LC12 bathymetries compared to the SRTM. Both the WOLP and the LC12 exhibit similar hypsometry in depths of <1 m (dissimilar to the SRTM). According to these maps, the southwestern sub-basin (Belt Bay) is the first to be filled (in accordance with MODIS imagery of floods, Supplementary movie 1 [SM1]). Differences between WOLP and LC12 bathymetries increase above lake depths of 1 m, when the southeastern sub-basin (Madigan Gulf) fills according to WOLP bathymetry. In the LC12 map, the sill between the southern sub-basins is higher and therefore the flooded area increases only above water depth of 2 m. Large differences exist between WOLP and LC12 at the lake's margins; there, LC12 bathymetry rises ~5 m above the lake bottom (Figure 3a). These differences seem to be related to the SRTM-dependent mapping of the lake margins in LC12. At a depth of 3.1 m, the WOLP flooded area reaches its maximum extent, featuring an area of 6.1×10^3 km^2 and a volume of 8.9 km^3, ~33% higher than the respective area and volume calculated based on the LC12 map (Figure 3a). Nevertheless, it is important to note that WOLP bathymetry represents only regions that were flooded between 1984 and 2015, and that the largest flood in recent history occurred in the 1970's. Therefore higher shorelines, as in LC12 or Cohen et al. (2018), could not be mapped with WOLP.

4 Application for non-mapped and inundated lakes

Sabkhat El-Mellah is a small, northwestern Sahara ephemeral lake (~170 km^2) (Figure 2e, f). It is fed in the High Atlas Mountains and is flooded only once every few years (Mabbutt, 1977). There is no bathymetric map of this lake that we are aware of. A comparison of the WOLP bathymetry (Figure S5) to the SRTM data (Figures 2d, S6) indicates generally a similar pattern (location of the deepest part of the lake and its margins, large scale slopes, etc.). However, variations of the SRTM data over Sabkhat El-Mellah are approximately ±2 m (Figures 3b, S6), while lake

depth is ~5 m, yielding an uncharacteristic discontinuous and rough lake floor (e.g., Quade et al., 2018). The mean cross-validation RMSD of WOLP bathymetry is much lower (0.32 m; Table 1, Figure S7). The WOLP map exhibits a much higher flooded area in comparison with the SRTM data (Figure 3b). E.g., at a 1 m lake depth, the WOLP lake area is 0.15×10^3 km^2 versus 0.08×10^3 km^2 according to SRTM data.

The same methodology was applied over Lago Coipasa (or Salar de Coipasa; surface area up to 2400 km^2), which is a high altitude (3660 m), shallow saline lake, occasionally filled with water (Placzek et al., 2006) (Figure 2e, i). However, during February 2019, the lake was flooded (SM2), thus, ICESat-2 scans taken afterward exhibit both the water surface and the lake floor in its inundated region.

Recent studies highlight the ability of ICESat-2 scans to penetrate water and yield bathymetric profiles (Forfinski-Sarkozi and Parrish, 2016; Ma et al., 2019; Parrish et al., 2019). Therefore, we derived two different bathymetric maps of Lago Coipasa, one using all available "dry" scans (i.e., before February 2019; Figure S8), and the other (Figure S9) using only post-flood scans ("wet" scans), manually omitting the ICESat-2's water surface readings (SI3). The difference between the "dry" bathymetry and the SRTM data, and the difference between the "dry" and "wet" maps are shown in Figures 2g and 2h, respectively. Given the difficulty in determining water density, we did not correct the effect of the changing refraction coefficient between water and air on underwater elevation measurements. However, to avoid location errors, we used only nadir data, which are expected to have the least spatial error. The expected vertical error where water depth is ~0.7 m (SI3), as in this 2019 flood, is <0.18 m (Parrish et al., 2019) or even less (as shown in Ma et al., 2019).

Similar to Lake Eyre, the WOLP-SRTM difference map (Figure 2g) illustrates that Lago Coipasa was inundated during the SRTM scan, and the wet part of the scan was replaced with a fixed elevation value. The SRTM data over the lake area varies within ~±5 m (RMSD=2.84 m; Figures 3c and S10), meaning that over a ~1.5 m deep lake, such as Lago Coipasa, SRTM-based water volume calculations for all practical matters are absurd. In contrast, both the "dry" and the "wet" WOLP bathymetries yield a much smaller mean cross-validation RMSD value (0.28 m and 0.47 m, respectively; Table 1, Figures S11, S12).

The fixed-elevation polygon in the SRTM data for Lago Coipasa is bounded by high (>2 m) artificial walls. This is exhibited in the hypsometry by a sharp increase and then a fixed wetted area of 0.87×10^3 km^2 (Figure 3c). In lake depths of <1 m, the "dry" bathymetry presents a detailed gradual increase in lake area and volume, filling most of the maximum lake extent. The "wet" WOLP area at 1 m depth is smaller than the "dry" area due to a 1.3 m deeper lake bottom in the "wet" bathymetry (Figure 3c; SI2). Both the "dry" and "wet" scans did not cross the northernmost part of the lake, which is characterized by the highest water occurrence (and presumably deepest water column). For this reason, we stress that future crossing of ICESat-2 over this specific region of the lake could improve its bathymetry.

Compared with the "dry" bathymetry, 58% of the "wet" lake area lies within ±0.5 m of the "dry" bathymetry (RMSD = 0.39 m). Thus, relying on the "dry" bathymetric map, which seems reasonable in light of the results shown for Lake Eyre, we suggest that even when using only the "wet" scans, the WOLP bathymetry yields better results than the currently available global product (SRTM). This leads us to propose the usage of the methodology presented here for any of the world's shallow desert lakes.

5 Discussion

The largest source of uncertainty in the WOLP bathymetry stems from the selected fitting equation between water occurrence and elevation (step c). However, this selection affects mainly the extremities of data, i.e., the extrapolation of elevation to values that were not observed by the ICESat-2 (areas with gray dots in Figures 1c, S5, S8, S9). Thus, in cases where ICESat-2 data covers the water frequency extremities, WOLP bathymetry is accurate, as demonstrated by the cross-validation results. Large enough lakes should be covered by at least a few ICESat-2 scans (e.g., Figure 1a) and therefore, scans are expected to cover a wide range of water occurrences. This wide range can yield an accurate bathymetry for almost all of the lake extent.

Laser altimetry errors, estimated to be ~0.3 m for a single photon return, and much lower (0.05-0.07 m) for an average of neighboring photon returns (Jasinski et al., 2016), are not expected to impact our results significantly. A larger uncertainty lies between points that have a similar water occurrence but different elevation, as is the case if there are small and local topographic minima. Using more scans may decrease the variations, although some of them may be intrinsic, e.g., where transmission-losses or springs are common. Water occurrence minima can be too small to be identified as a different sub-basin. Thus, our method is limited to sub-basins that are large enough to be resolved with ICESat-2, as in Lake Eyre (Figure 1, SI1). In deriving the Lake Eyre bathymetry, we used at least four scans for each sub-basin, yielding an error of only 0.2-0.6 m (Table 1, Figure S4).

Another limitation to our methodology comes from the maximum water penetration of the ICESat-2 laser. This limits the ability to derive bathymetry in lakes that have a water depth of tens of meters or more. In such circumstances, a partial bathymetry could still be derived for the outskirts of the lakes using our methodology, or as presented in Li et al. (2019) or in Ma et al. (2019) for the shoulders of Lake Mead. However, we focus here on shallow desert lakes, in which, by definition, this is not a major obstacle.

Sediment deposition could also increase the uncertainty of the derived bathymetry. Here, we use satellite imaging water occurrence from >30-yr period (Pekel et al., 2016), implying that if the lake floor was altered during this time interval, present-day ICESat-2 scans can yield only an averaged bathymetry of this period. However, newer global water occurrence datasets could emerge in the near future, enabling both derivation of newer bathymetries, and higher resolution maps (e.g., 10-20 m pixels from Sentinel-2).

Apart from these limitations, taking a long series of satellite imagery extends a great opportunity. If only specific dates are used to identify isobaths (or shorelines), the error propagates to the bathymetric map. Using statistics based on many years, single image errors diminish. Such errors include water piling-up on one side of the lake due to winds (Arsen et al., 2013), misclassification of water boundaries or crossing isobaths (Long et al., 2019), and specific date imaging having only partial coverage of a lake, because of imaging geometry or cloud obscuration. Moreover, the use of specific date imagery requires a spatial interpolation between isobaths, thus concealing small features in between isobaths.

Out of the three lakes analyzed above, Lake Eyre is probably the most closely monitored, yet the nearest river gauge is situated many hundreds of kilometers upstream. Therefore, there is no accurate in-situ data for water input volumes. ICESat-2's high spatial resolution (~70 cm) combined with high-resolution water occurrence map (e.g., 30 m in the map of Pekel et al., 2016) yields an accurate, high-resolution bathymetry, even over flooded or complex desert lakes. Such maps could help in determining the water discharge into remote desert lakes and their evaporative losses, providing much-needed data in remote areas, serving as a basis for mass and energy balance calculations over such lakes, and for water management strategies.

6 Conclusions

Using a new methodology which links long-term water occurrence and accurate height measurements, each independently derived from satellite remote-sensing, we mapped the bathymetry of three shallow lakes in drylands across the globe. We verified the bathymetries using a previous bathymetric map, SRTM data, and through cross-validation. This easy-to-implement methodology yields a high-resolution bathymetry of shallow desert lakes that were flooded sometime during 1984-2015, using globally available datasets.

- As an example of a complex shallow lake system, we used Lake Eyre, consisting of multiple sub-basins. Despite its complexity, verification versus the best available DEM showed that the methodology is successful, as long as each sub-basin is covered by an elevation measurement scan.
- The methodology was also applied to two lakes with no previous bathymetry maps, one in the Sahara (Sabkhat El-Mellah) and the other in the Altiplano (Lago Coipasa). Results proved low cross-validation RMSD values (~0.3 m) compared with the SRTM data (~2.5 m).
- Applying the methodology in Lago Coipasa separately to "dry" and to "wet" ICESat-2 scans, relying on laser penetrability, we showed that bathymetry can even be produced during lake inundation.

The presented methodology can be applied to a large portion of the shallow lakes around the globe. It enables mapping of inundated lakes (a major obstacle for widely used methods), small lakes, and large and complex lake systems.

Acknowledgments and Data

This research was supported by ISF grant 946/18 and NSFC-ISF grant 2487/17 to YE. Water occurrence data (Pekel et al., 2016) were obtained from https://global-surface-water.appspot.com, using Google Earth Engine (https://earthengine.google.com/). ICESat-2 ATL03 data were obtained from https://openaltimetry.org/data/icesat2/: Neumann, T. A., A. Brenner, D. Hancock, J. Robbins, J. Saba, K. Harbeck, and A. Gibbons. 2019. ATLAS/ICESat-2 L2A Global Geolocated Photon Data, V1. [ATL03]. Boulder, Colorado USA. NSIDC: National Snow and Ice Data Center. doi: https://doi.org/10.5067/ATLAS/ATL03.001. [Dec 2019]. The authors declare no conflict of interests.

References

Arsen, A., Crétaux, J. F., Berge-Nguyen, M. and del Rio, R. A.: Remote sensing-derived bathymetry of Lake Poopó, Remote Sens., 6(1), 407–420, doi:10.3390/rs6010407, 2013.

Berry, P. A. M., Garlick, J. D. and Smith, R. G.: Near-global validation of the SRTM DEM using satellite radar altimetry, Remote Sens. Environ., 106(1), 17–27, doi:10.1016/j.rse.2006.07.011, 2007.

Brenner, A. C., DiMarzio, J. P. and Zwally, H. J.: Precision and accuracy of satellite radar and laser altimeter data over the continental ice sheets, IEEE Trans. Geosci. Remote Sens., 45(2), 321–331, doi:10.1109/TGRS.2006.887172, 2007.

Brunt, K. M., Neumann, T. A. and Smith, B. E.: Assessment of ICESat-2 Ice Sheet Surface Heights, Based on Comparisons Over the Interior of the Antarctic Ice Sheet, Geophys. Res. Lett., 46, 13072–13078, doi:10.1029/2019GL084886, 2019.

Bye, J. A. T., Dillon, P. J., Vandenberg, J. C. and Will, G. D.: Bathymetry of Lake Eyre, Trans. R. Soc. South Aust., 102(1), 85–89, doi:10.1080/00359196009519029, 1978.

Cohen, T. J., Jansen, J. D., Gliganic, L. A., Larsen, J. R., Nanson, G. C., May, J. H., Jones, B. G. and Price, D. M.: Hydrological transformation coincided with megafaunal extinction in central Australia, Geology, 43(3), 195–198, doi:10.1130/G36346.1, 2015.

Cohen, T. J., Meyer, M. C. and May, J. H.: Identifying extreme pluvials in the last millennia using optical dating of single grains of quartz from shorelines on Australia's largest lake, Holocene, 28(1), 150–165, doi:10.1177/0959683617715700, 2018.

Crétaux, J. F., Abarca-del-Río, R., Bergé-Nguyen, M., Arsen, A., Drolon, V., Clos, G. and Maisongrande, P.: Lake Volume Monitoring from Space, Surv. Geophys., 37(2), 269–305, doi:10.1007/s10712-016-9362-6, 2016.

D'Odorico, P. and Porporato, A.: Dryland ecohydrology., 2006.

Enzel, Y. and Wells, S. G.: Extracting Holocene paleohydrology and paleoclimatology information from modern extreme flood events: An example from southern California, Geomorphology, 19(3–4), 203–226, doi:10.1016/s0169-555x(97)00015-9, 1997.

Feng, L., Hu, C., Chen, X., Li, R., Tian, L. and Murch, B.: MODIS observations of the bottom topography and its inter-annual variability of Poyang Lake, Remote Sens. Environ., 115(10), 2729–2741, doi:10.1016/j.rse.2011.06.013, 2011.

Forfinski-Sarkozi, N. A. and Parrish, C. E.: Analysis of MABEL bathymetry in Keweenaw Bay and implications for ICESat-2 ATLAS, Remote Sens., 8(9), doi:10.3390/rs8090772, 2016.

Gao, H.: Satellite remote sensing of large lakes and reservoirs: from elevation and area to storage, Wiley Interdiscip. Rev. Water, 2(2), 147–157, doi:10.1002/wat2.1065, 2015.

Jasinski, M. F., Stoll, J. D., Cook, W. B., Ondrusek, M., Stengel, E. and Brunt, K.: Inland and Near-Shore Water Profiles Derived from the High-Altitude Multiple Altimeter Beam Experimental Lidar (MABEL), J. Coast. Res., 76, 44–55, doi:10.2112/si76-005, 2016.

Jawak, S. D., Vadlamani, S. S. and Luis, A. J.: A Synoptic Review on Deriving Bathymetry Information Using Remote Sensing Technologies: Models, Methods and Comparisons, Adv. Remote Sens., 04(02), 147–162, doi:10.4236/ars.2015.42013, 2015.

Kotwicki, V. and Isdale, P.: Hydrology of Lake Eyre, Australia: El Niño link, Palaeogeogr. Palaeoclimatol. Palaeoecol., 84(1–4), 87–98, doi:10.1016/0031-0182(91)90037-R, 1991.

Leon, J. X. and Cohen, T. J.: An improved bathymetric model for the modern and palaeo Lake Eyre, Geomorphology, 173–174, 69–79, doi:10.1016/j.geomorph.2012.05.029, 2012.

Li, Y., Gao, H., Jasinski, M. F., Zhang, S. and Stoll, J. D.: Deriving High-Resolution Reservoir Bathymetry From ICESat-2 Prototype Photon-Counting Lidar and Landsat Imagery, IEEE Trans. Geosci. Remote Sens., PP(June), 1–11, doi:10.1109/tgrs.2019.2917012, 2019.

Long, Y., Yan, S., Jiang, C., Wu, C., Tang, R. and Hu, S.: Inversion of Lake Bathymetry through Integrating Multi-Temporal Landsat and ICESat Imagery, Sensors, 19(13), 2896, doi:10.3390/s19132896, 2019.

Ma, Y., Xu, N., Sun, J., Wang, X. H., Yang, F. and Li, S.: Estimating water levels and volumes of lakes dated back to the 1980s using Landsat imagery and photon-counting lidar datasets, Remote Sens. Environ., 232(July), 111287, doi:10.1016/j.rse.2019.111287, 2019.

Mabbutt, J. A.: Desert landforms, Second pri., The MIT Press, Cambridge, Massachusetts, USA., 1977.

Markus, T., Neumann, T., Martino, A., Abdalati, W., Brunt, K., Csatho, B., Farrell, S., Fricker, H., Gardner, A., Harding, D., Jasinski, M., Kwok, R., Magruder, L., Lubin, D., Luthcke, S., Morison, J., Nelson, R., Neuenschwander, A., Palm, S., Popescu, S., Shum, C. K., Schutz, B. E., Smith, B., Yang, Y. and Zwally, J.: The Ice, Cloud, and land Elevation Satellite-2 (ICESat-2): Science requirements, concept, and implementation, Remote Sens.

Environ., 190, 260–273, doi:10.1016/j.rse.2016.12.029, 2017.
de Martonne, E.: Regions of Interior-Basin Drainage, Geogr. Rev., 17(3), 397–414, 1927.
New, M., Lister, D., Hulme, M. and Makin, I.: A high-resolution data set of surface climate over global land areas, Clim. Res., 21(1), 1–25, doi:10.3354/cr021001, 2002.
Nicholson, S. E.: Dryland climatology, Cambridge University Press, New York., 2011.
Noy-Meir, I.: Desert Ecosystems: Environment and Producers, Annu. Rev. Ecol. Syst., 4, 25–51, 1973.
Parrish, C. E., Magruder, L. A., Neuenschwander, A. L., Forfinski-Sarkozi, N., Alonzo, M. and Jasinski, M.: Validation of ICESat-2 ATLAS Bathymetry and Analysis of ATLAS's Bathymetric Mapping Performance, Remote Sens., 11(14), 1634, doi:10.3390/rs11141634, 2019.
Pekel, J. F., Cottam, A., Gorelick, N. and Belward, A. S.: High-resolution mapping of global surface water and its long-term changes, Nature, 540(7633), 418–422, doi:10.1038/nature20584, 2016.
Placzek, C., Quade, J. and Patchett, P. J.: Geochronology and stratigraphy of late Pleistocene lake cycles on the southern Bolivian Altiplano: Implications for causes of tropical climate change, Bull. Geol. Soc. Am., 118(5–6), 515–532, doi:10.1130/B25770.1, 2006.
Quade, J., Dente, E., Armon, M., Ben Dor, Y., Morin, E., Adam, O. and Enzel, Y.: Megalakes in the Sahara? A Review, Quat. Res. (United States), 90(2), 253–275, doi:10.1017/qua.2018.46, 2018.
Schwanghart, W. and Scherler, D.: Short Communication: TopoToolbox 2 - MATLAB-based software for topographic analysis and modeling in Earth surface sciences, Earth Surf. Dyn., 2(1), 1–7, doi:10.5194/esurf-2-1-2014, 2014.
Sun, F. and Ma, R.: Hydrologic changes of Aral Sea: A reveal by the combination of radar altimeter data and optical images, Ann. GIS, 25(3), 247–261, doi:10.1080/19475683.2019.1626909, 2019.
UNEP: World atlas of desertification, London : Edward Arnold, London., 1992.

Figures and table

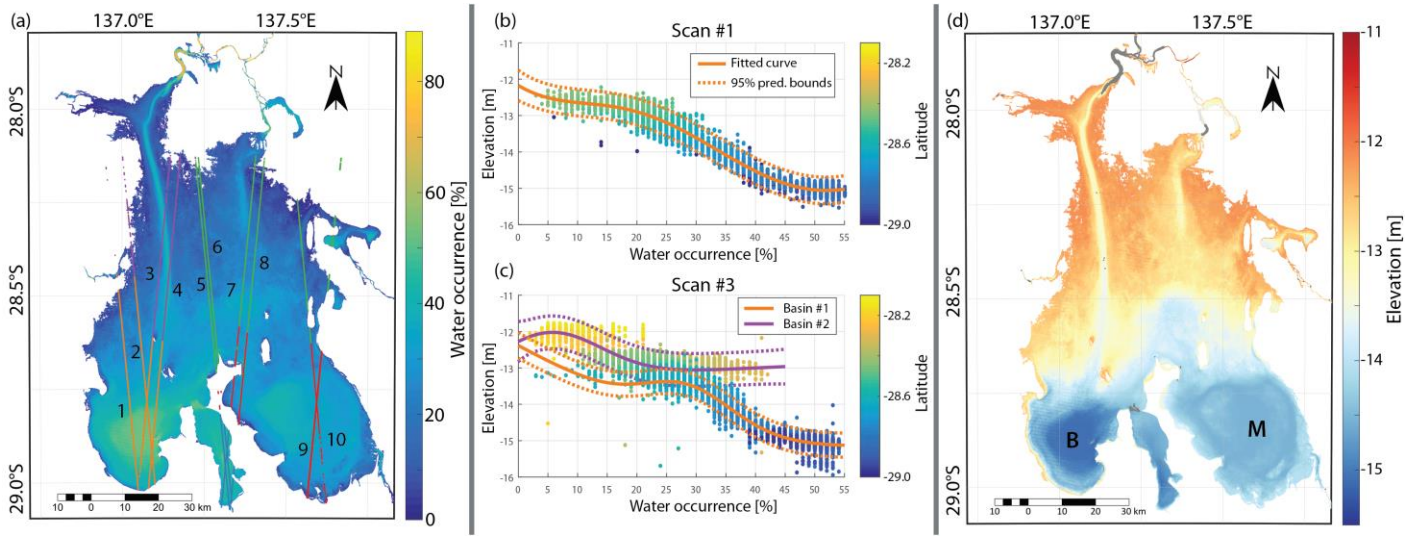

Figure 1. An example of bathymetry derivation in Lake Eyre North (a schematic representation of this process is in Fig S1). (a) Water occurrence from Pekel et al. (2016) and ten ICESat-2 scans over the lake (labeled) used to derive elevations. Scans are colored by the 5 identified pseudo-watersheds (SI1). (b) The relation between water occurrence and elevation measurements from ICESat-2 scan #1 with a two-term gaussian fit and its 95% prediction boundaries. Colors represent latitude. (c) The same as in b, but for scan #3. The fit here is divided according to the watersheds. (d) Derived bathymetry map based on the methodology presented in Section 2. Gray dots represent regions in which water occurrence is greater than the highest occurrence overpassed by ICESat-2. B = Belt Bay. M = Madigan Gulf.

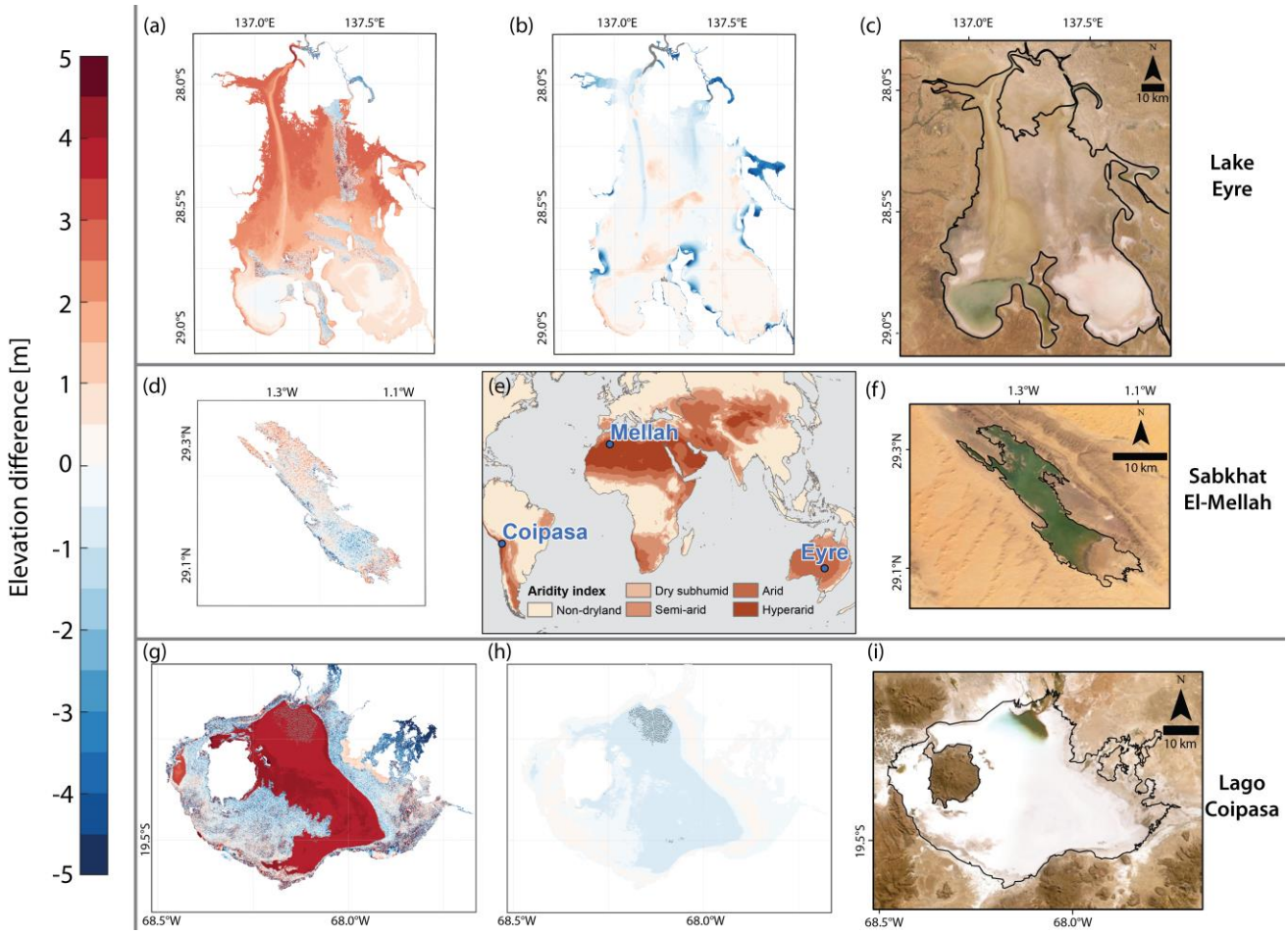

Figure 2. Comparisons of WOLP bathymetries with SRTM data in Lake Eyre (a), Sabkhat El-Mellah (d), and Lago Coipasa (g). (b) Comparison of Lake Eyre bathymetry with the map of Leon & Cohen (2012). (e) Location map of the three lakes, and aridity index (UNEP, 1992) from the Climatic Research Unit of the University of East Anglia (New et al., 2002). True-color satellite imagery of the lakes from Esri\Digitalglobe, and maximum extent of water occurrence in black) from Pekel et al. (2016) (c, f, i). (h) Difference between the "wet" and "dry" bathymetries of Lago Coipasa.

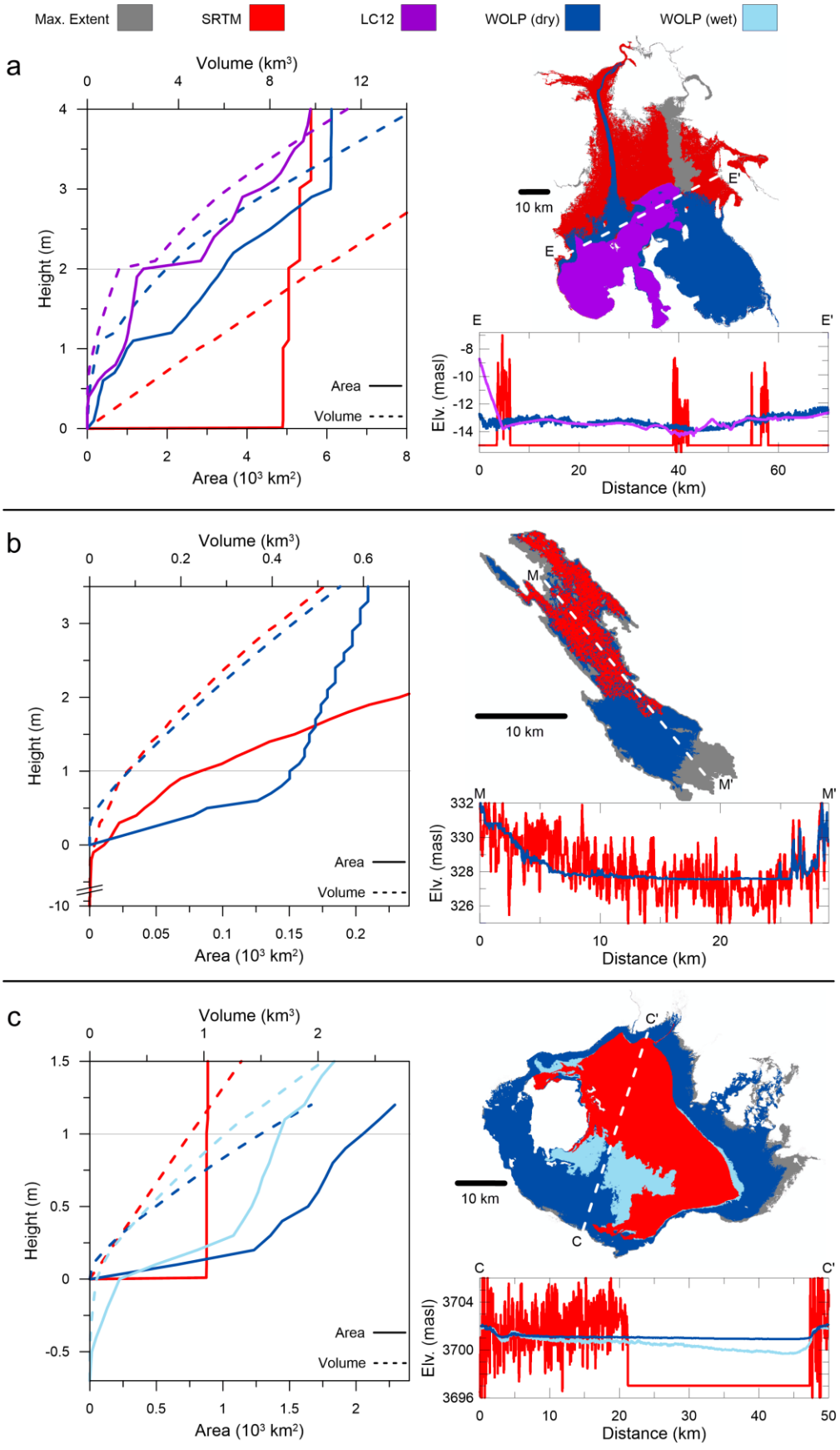
Max. Extent
SRTM
LC12
WOLP (dry)
WOLP (wet)
a
Volume (km³)
Height (m)
Area
Volume
Area (10³ km²)
10 km
E
E'
Elv. (masl)
Distance (km)
b
M
M'
c
C
C'

354

355 **Figure 3**. Hypsometric curves, extent maps and cross-sections for Lake Eyre (a), Sabkhat El-
356 Mellah (b), and Lago Coipasa (c). The maps show filling extent at heights (denoted by a gray
357 line on the hypsometric curves) that exert major differences between bathymetries. Details of the
358 preparation of the hypsometries are in SI2.
359

360 **Table 1.** *Validation results across the lakes*

Lake	Validated map	Reference	Regional / Profile validation	RMSD [m]	Lake depth [m]
Lake Eyre	SRTM	LC12	Regional	1.77	3.2 (WOLP) §, 4.1 (LC12) §
	WOLP (this study)	LC12	Regional	0.52	
	SRTM	ICESat-2	Profile	0.95-2.30*	
	LC12	ICESat-2	Profile	0.20-0.69*	
	WOLP	ICESat-2	Profile, cross-validation	0.21-0.57*	
Sabkhat El-Mellah	SRTM	ICESat-2	Profile	2.04#	5.0 (WOLP)§
	WOLP	ICESat-2	Profile, cross-validation	0.32#	
Lago Coipasa	SRTM	ICESat-2	Profile	2.84#	1.2 (WOLP: "dry")§
	WOLP ("dry")	ICESat-2	Profile, cross-validation	0.28#	
	WOLP ("wet")	WOLP ("dry")	Regional	0.39	2.2 (WOLP: "wet")§
	WOLP ("wet")	ICESat-2	Profile, cross-validation	0.47#	

361 *Range denotes the average RMSD for each sub-basin, averaged between the different ICESat-2 profiles in it.
362 #Average among the different ICESat-2 profiles.
363 §Estimated (see SI2).
364

Geophysical Research Letters

Supporting Information for

Determining bathymetry of shallow and ephemeral desert lakes using satellite imagery and altimetry

M. Armon[1], E. Dente[1,2,3], Y. Shmilovitz[1,2], A. Mushkin[2], T. J. Cohen[4], E. Morin[1], and Y. Enzel[1]

[1]The Fredy and Nadine Herrmann Institute of Earth Sciences, the Hebrew University of Jerusalem, Israel.

[2]The Geological Survey of Israel, Israel.

[3]Shamir Research Institute, University of Haifa, Israel.

[4]School of Earth and Environmental Sciences, University of Wollongong, Australia.

Contents of this file

Additional Supporting Information (Files uploaded separately)

Introduction

This supporting information file includes an explanation about the usage of water occurrence to divide Lake Eyre to sub-basins, and the neighborhood-weighting of pixel elevation values in it (text S1). This is followed by a description of the derivation of hypsometric curves (text S2) and of the usage of "wet" elevation measurements in Lago Coipasa (text S3). The figures at the end of this file (Figures S1-S14), and the attached movies (S1-S2) present additional features of the WOLP bathymetry methodology (elevation cross-sections, bathymetry maps not shown in the main text, etc.) and provide the specific ICESat-2 scan dates.

Text S1. Lake Eyre sub-basin division and neighborhood weighting of elevation values

1) Dividing Lake Eyre into sub-basins

Small variations in lake floor height in shallow and vast lakes are often manifested as several sub-basins. Such lakes show a complex relation of water occurrence and elevation (e.g., Figure 1c). To overcome this complexity, different sub-basins should be represented by different relations. We extracted sub-basins of Lake Eyre North using pseudo watersheds obtained from the water occurrence map (Figure 1a) in a similar manner to topographic analyses; routines of flow directions and fill were performed on the map of water occurrence residue from 100% using the TopoToolbox V2 (Schwanghart and Scherler, 2014). To use this approach, one must make sure the division into sub-basins meets two conditions (1) at least one (and preferably more) ICESat-2 scan overpassed the sub-basin, (2) the division into several drainage basins seems realistic (e.g., by comparison to satellite images; e.g., Movie S1). We found the division into five sub-basins in Lake Eyre North is an optimal balance between these two conditions (Figure S2). Specifically, we ensured at least four ICESat-2 scans in each sub-basin.

2) Neighborhood weighting of values in Lake Eyre

The relation between water occurrence and elevation in Lake Eyre (Section 3) was calculated separately for each of the sub-basins. Such calculation yields a step-like topography (Figure S13), at the boundaries of each basin. To avoid both this step, and the high sensitivity in elevation of each pixel to the exact sub-basin division, regions closer than ~11 km (400 pixels distance) to the pseudo water divide were assigned values from neighboring basins as well, inversely weighted according to their distance from the divide. The elevations near sub-basin boundaries were calculated using the following averaging, yielding the elevation of each pixel (h_i):

$$\begin{cases} d^*_{i,j} = 1 - \frac{d_{i,j}}{D}, & d_{i,j} < D \\ d^*_{i,j} = 0, & d_{i,j} \geq D \end{cases} \quad \text{(Eq. S1)}$$

$$w_i = \sum_{j=1}^{n} d^*_{i,j} \quad \text{(Eq. S2)}$$

$$h_i = \frac{1}{w_i} \sum_{j=1}^{n} h_{i,j} \cdot d^*_{i,j} \quad \text{(Eq. S3)}$$

where i is the pixel id, j is the sub-basin id, D is the maximum distance used for averaging, $d_{i,j}$ is the distance (number of pixels) between pixel i and the closest pixel in the j^{th} watershed, $h_{i,j}$ is the elevation calculated using the specific j^{th} sub-basin fit (as detailed in Section 2), n is the number of sub-basins, and w_i is the sum of weights ($d^*_{i,j}$) given to pixel i because of its proximity to watershed boundaries. Notice that if $d_{i,j} \geq D$ (i.e., when a pixel is farther from the watershed than the maximum distance for averaging) this calculation yields the same number as in a single watershed calculation ($h_{i,j}$). Namely, we consider this pixel as belonging to a single sub-basin.

Text S2. Calculations of the hypsometric curves and maximum lake depths

To calculate the hypsometric curves of the different lakes, a series of constant-value rasters were generated for each bathymetry (WOLP, SRTM, and LC12), with an elevation greater than the minimum elevation of the analyzed bathymetry. The increments of the constant-value rasters are 0.1 m. The bathymetries were kept in their original resolution (~30 m), without any

smoothing or sink filling. To calculate the area and volume of the lakes at different elevations, the ESRI ArcMap Cut-and-Fill tool was applied. Only the largest continuous area and the volume associated with it were extracted for each elevation. This methodology was chosen to simulate hydrologic connectivity during lake filling, and to clean out the filling of isolated regions within the bathymetry maps. Thus, the results of this procedure represent a filling stage of the lakes, rather than their desiccation stage.

In the northern and more frequently inundated area of Lago Coipasa, the "wet" bathymetric map features elevations that are lower than the "dry" WOLP map. These elevations were extrapolated, since no ICESat-2 scan passed through this region, and are therefore not identical. To have a common datum for the evaluation of the difference between the "wet" and the "dry" WOLP hypsometric curves of Lago Coipasa we shifted the height of the "wet" bathymetry by 0.7 m (negative values in Figure 3c). A similar procedure was applied to the SRTM map of Sabkhat El-Mellah, due to 10 m deep sinks in the original data.

Maximum lake depths were calculated based on WOLP bathymetry maps (and LC12 in Lake Eyre). The depths were derived from the difference between the minimum lake elevation and the elevation in which the area curves become asymptotic (i.e., the lake area reaches its maximum extent, based on data from Pekel et al., 2016) or the highest elevation of the bathymetric maps.

Text S3. Derivation of "wet" elevation scans in Lago Coipasa

Elevation measurements throughout this study are from the Advanced Topographic Laser Altimeter System (ATLAS) product #3 (ATL03) of the ICESat-2. Measurements used in the derivation of the bathymetry of Lago Coipasa were taken between October 2018 and May 2019 (Figure S8, S9). However, in February 2019 the lake was flooded (SM2).

The green light (532 nm) ATLAS measurements can give accurate water levels from the surface of a lake, however, they could also penetrate the water and give underwater floor elevation data in shallow environments (Parrish et al., 2019). A few methods to estimate which of the measurements are bottom readings exist. The basic idea is to derive the lowest data points that exhibit a continuous profile, which could either be done manually (Parrish et al., 2019), or using an algorithm accounting for the increased data point density at the lake bottom (Ma et al., 2019).

The difference in refraction coefficients between water and air yields an error in the horizontal geolocation of photon returns, which is minimized in nadiral photon returns (~9 cm for readings in water depth of 30 m; Parrish et al., 2019).

Parrish et al. (2019) provided an approximated equation to correct for the elevation difference in underwater photon returns:

$$Z' \approx Z + 0.25416D \qquad \text{(Eq. S4)}$$

where Z' is the corrected elevation, Z is the measured elevation, and D is the water depth, assuming a water refraction coefficient based on a temperature of 20°C and water salinity of 35 PSU (seawater). However, a freshwater salinity would yield roughly the same results (~0.5% difference).

To avoid horizontal offsets in this study, we use post-flood elevation data from only nadiral ATLAS profiles. Lake surface and water column data points were extracted manually, in places where the lake floor stands out (see an example for one scan profile in the figure below). To calculate the exact elevation, one needs to know the water depth, the angle between the laser beam and the water surface, and salinity and temperature of the water, most of which are hard to acquire in remote regions as Lago Coipasa. Because of the need for an optimization process

to find accurate water depths, and the relatively small bias expected when underwater corrections (Eq. S4) are applied, we did not correct this error. The expected bias due to a water depth of ~0.7 m, as in Lago Coipasa (see figure below) is <18 cm, which is still much lower than the SRTM data error (Table 1).

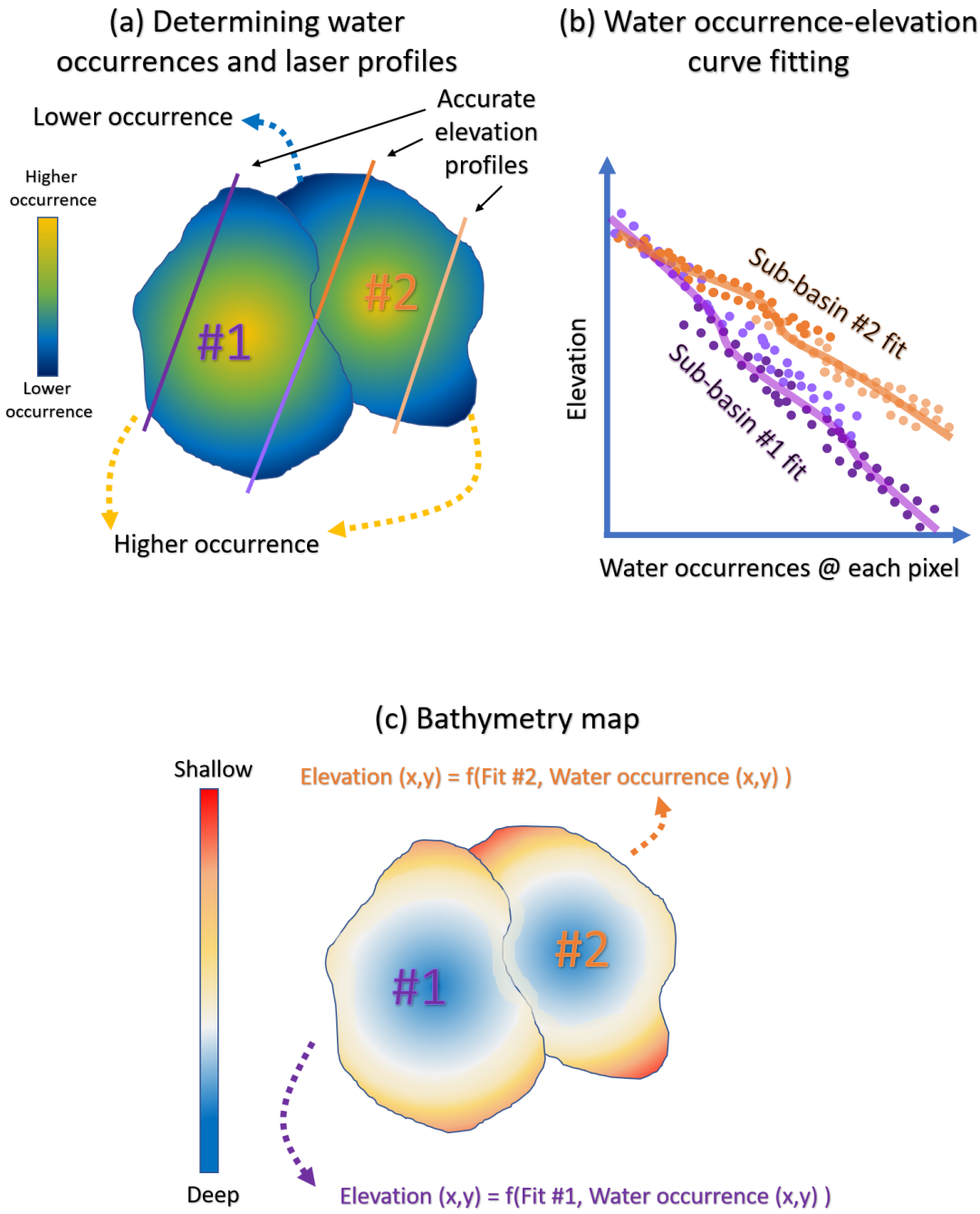

Figure S1. A schematic representation of the water occurrence-laser profiles (WOLP) method to derive bathymetries of shallow and ephemeral lakes. (a) Acquiring water occurrence from the global water occurrence map (Pekel et al., 2016) and ICESat-2 laser altimetry elevation data. Each laser profile is assigned to a specific sub-basin (marked in different colors). Pseudo sub-basins are identified using the water occurrence map. (b) Fitting occurrence-elevation curves for each of the sub-basins (#1 and #2) based on all laser altimetry profiles covering the specific sub-basin. (c) Application of the different fits for each sub-basin. The elevation at each pixel is determined by the fit of its assigned sub-basin, and by the water occurrence value at that pixel. Shallower bathymetry is inferred from low water occurrence values in individual

(~30 m) pixels during 1984-2015. Deeper bathymetry is inferred from high water occurrence. Please note the bathymetry is not directly related to the water-occurrence (compare the pattern of panels c and a), but rather to the obtained fits of each sub-basin.

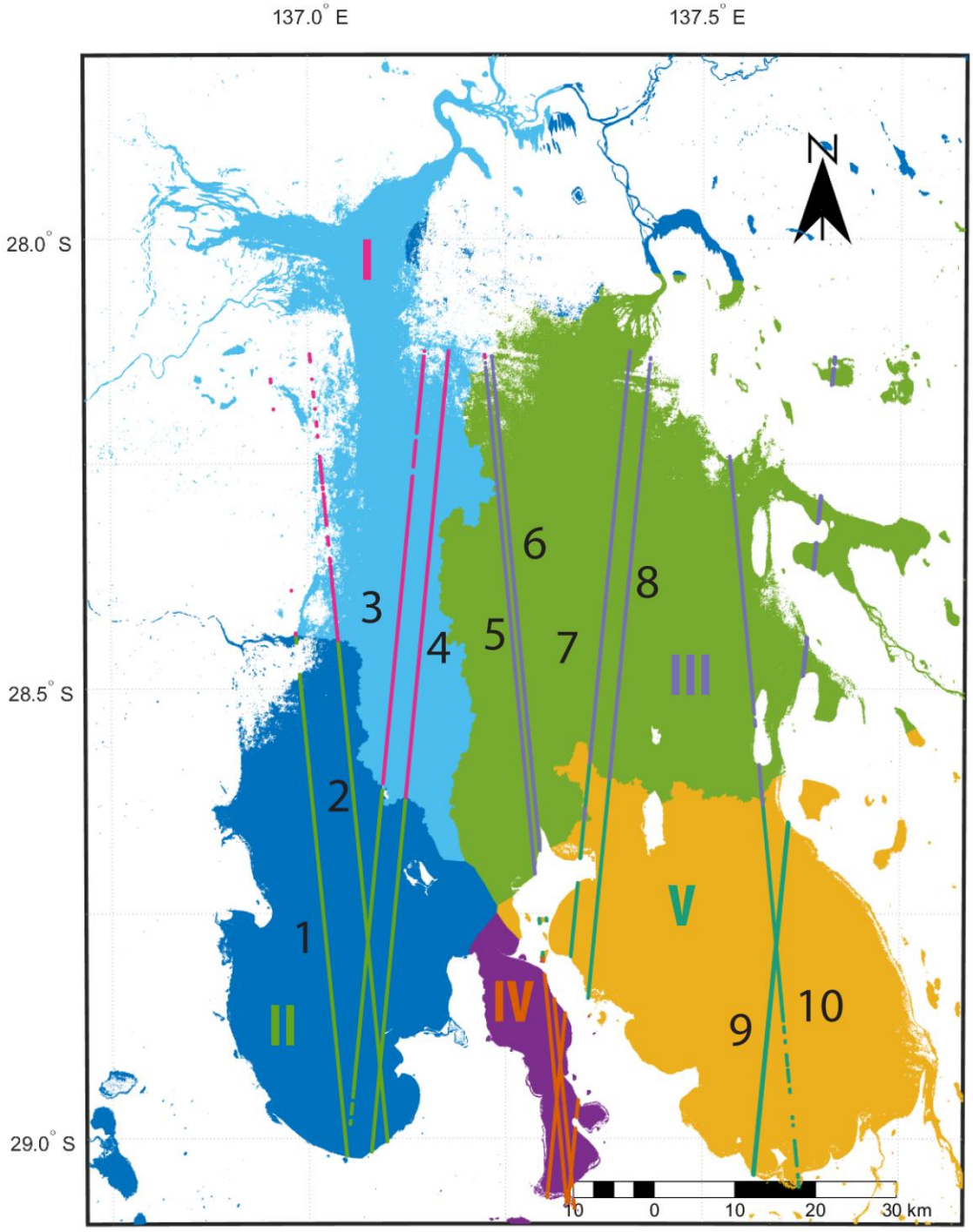

Figure S2. Sub-basins in Lake Eyre North (colored regions; labeled in Latin Numerals), and ICESat-2 scan profiles used in WOLP bathymetry derivation (labeled 1-10). Data from these scans were used according to their location in the various sub-basins. Scans 1-10 were taken during the following overpasses: 1 = 2019-03-06_t1046; 2 = 2018-12-06_t1046; 3 = 2018-11-20_t810; 4 = 2019-02-19_t810; 5 = 2019-04-04_t101; 6 = 2019-01-04_t101; 7 = 2018-12-

19_t1252; 8 = 2019-03-20_t1252; 9 = 2018-10-18_t307, 2019-04-18_t307; 10 = 2018-11-03_t543. Data were downloaded from: https://openaltimetry.org/data/icesat2/, from the ATL03 product: Neumann, T. A., A. Brenner, D. Hancock, J. Robbins, J. Saba, K. Harbeck, and A. Gibbons. 2019. ATLAS/ICESat-2 L2A Global Geolocated Photon Data, Version 1. Boulder, Colorado USA. NSIDC: National Snow and Ice Data Center. doi: https://doi.org/10.5067/ATLAS/ATL03.001. [last Accessed at 31/12/2019]. Note: only high confidence data points were used. WGS84 ellipsoid elevations were transformed into Australian Height Datum (Australian 2020 geoid) using Geoscience Australia website at: http://www.ga.gov.au/ausgeoid/.

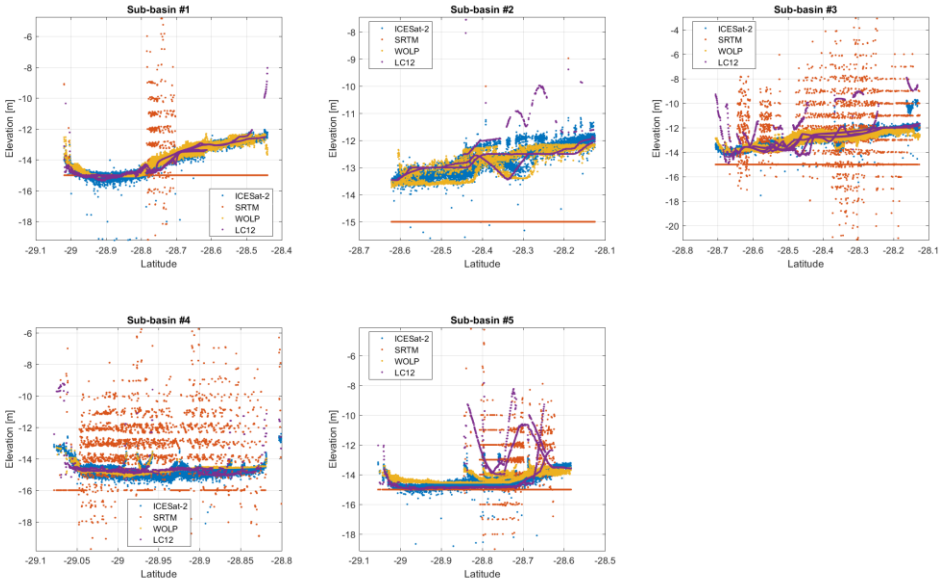

Figure S3. Elevations along ICESat-2 profiles at each of the sub-basins (Figure S2) of Lake Eyre from all data sources used in this study.

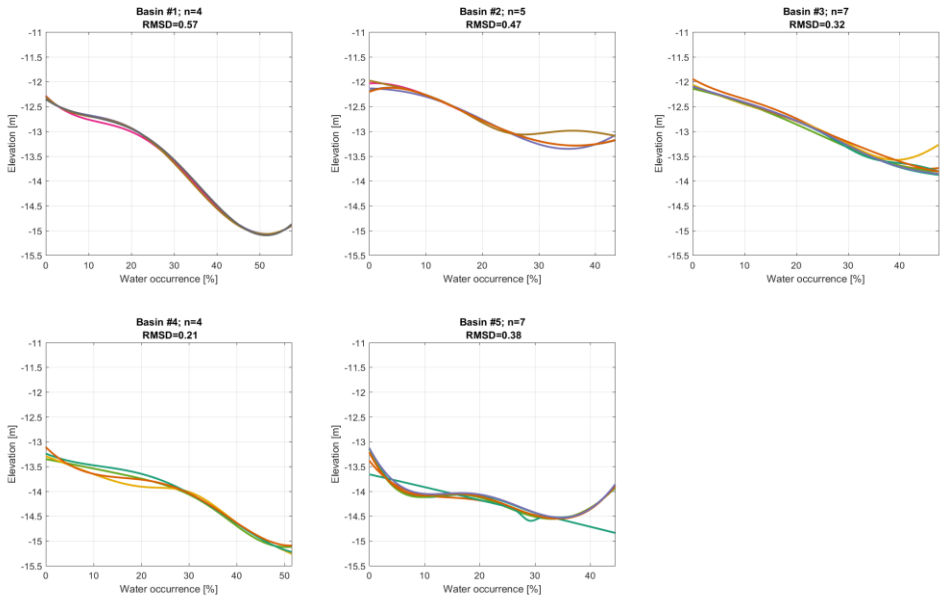

Figure S4. WOLP cross-validation results for each of the sub-basins (Figure S2) of Lake Eyre. Each curve is the 2-term Gaussian fit of ICESat-2 elevation data from all scans but one within a sub-basin, to water occurrence along scan profiles. The excluded scan was used to obtain RMSD values, and the average of these RMSD values is shown for each sub-basin. The number of scans for each sub-basin is denoted by "n".

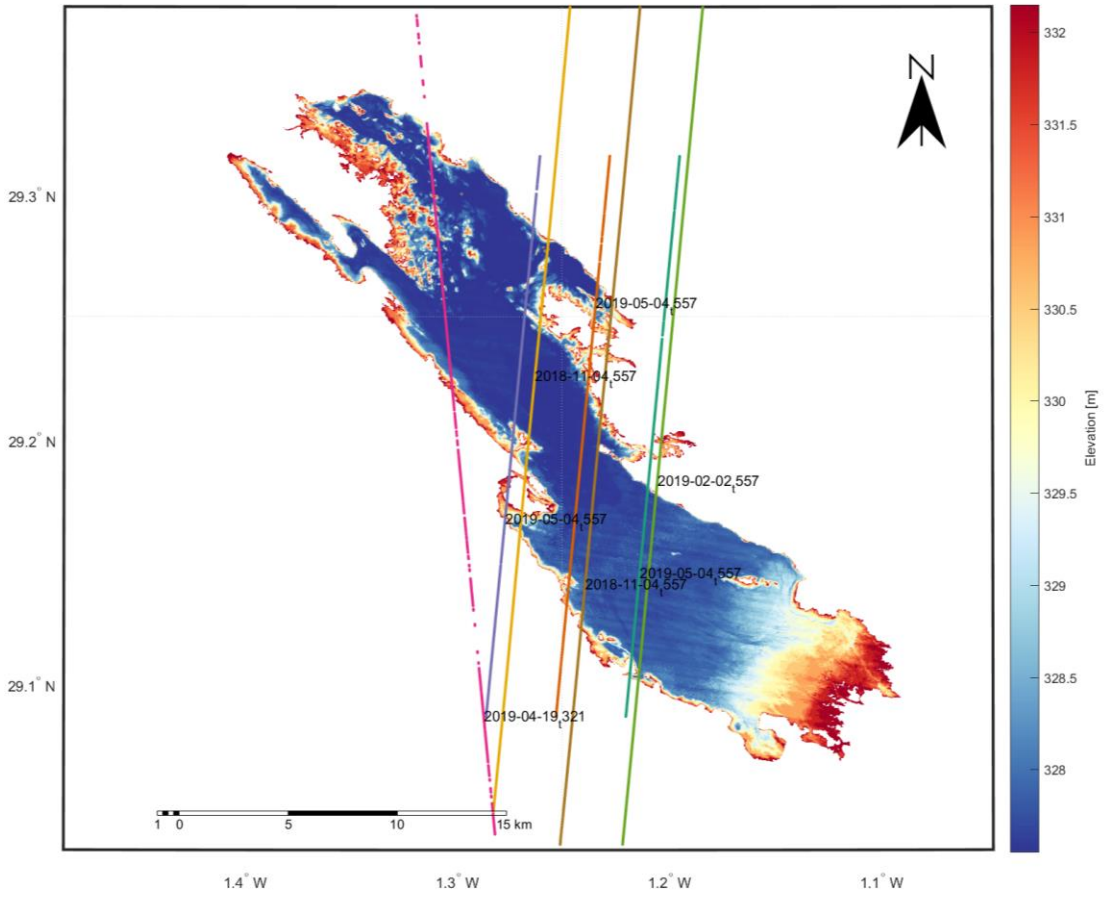

Figure S5. WOLP bathymetry of Sabkhat El-Mellah and ICESat-2 scans used to derive it. Scan dates and indices are listed next to each of the scans. Gray dots represent regions in which water occurrence is greater than the highest occurrence overpassed by ICESat-2.

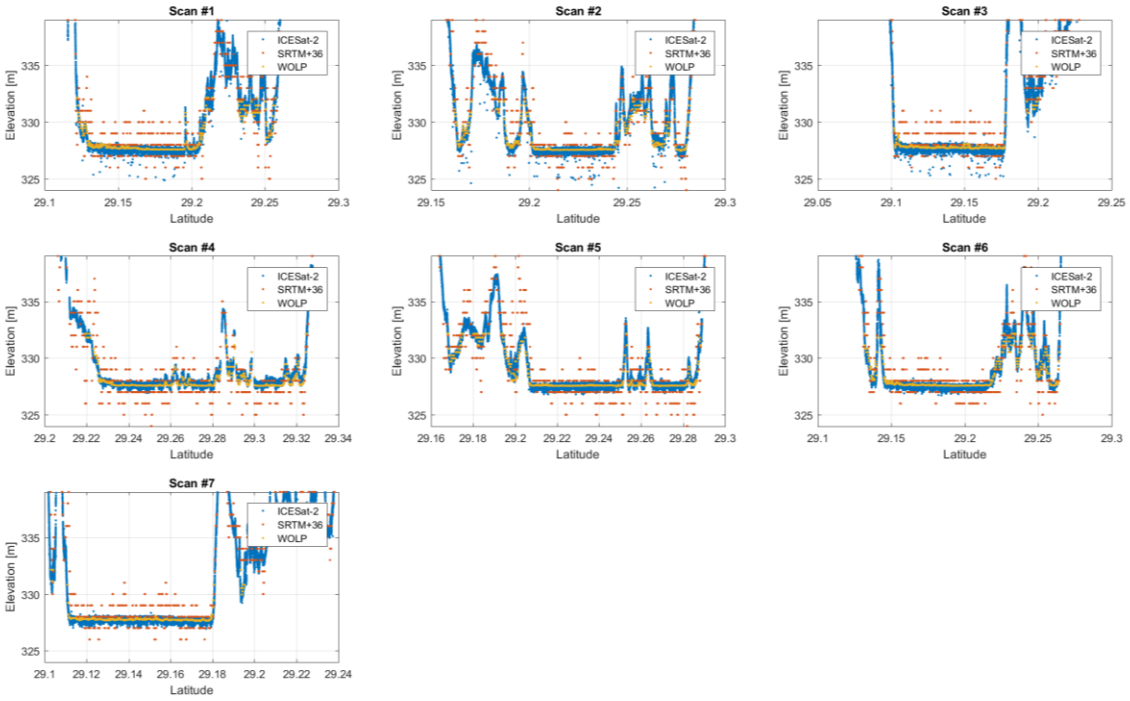

Figure S6. As in Figure S3, but for Sabkhat El-Mellah. SRTM elevation values were added a fixed correction value of 36 m, to compensate for the different vertical datum.

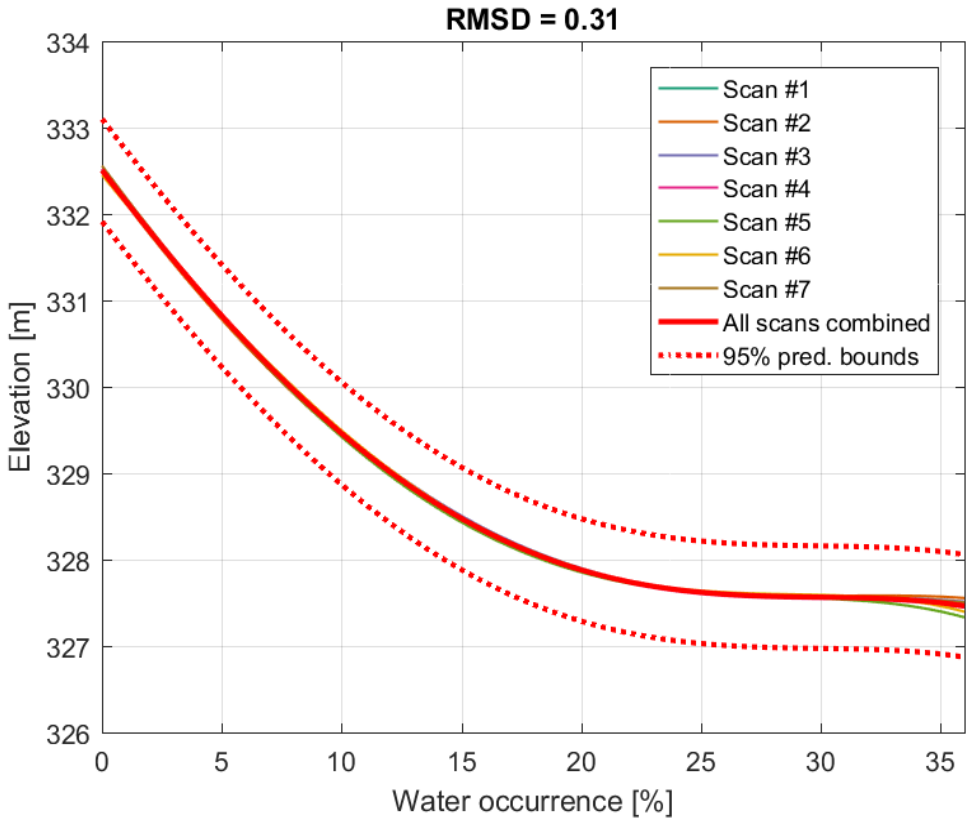

Figure S7. WOLP cross-validation results for Sabkhat El-Mellah. Each curve is the 2-term Gaussian fit of ICESat-2 elevation data from all scans but one, to water occurrence along scan profiles. The excluded scan was used to obtain RMSD values, and the average of these RMSD values is shown.

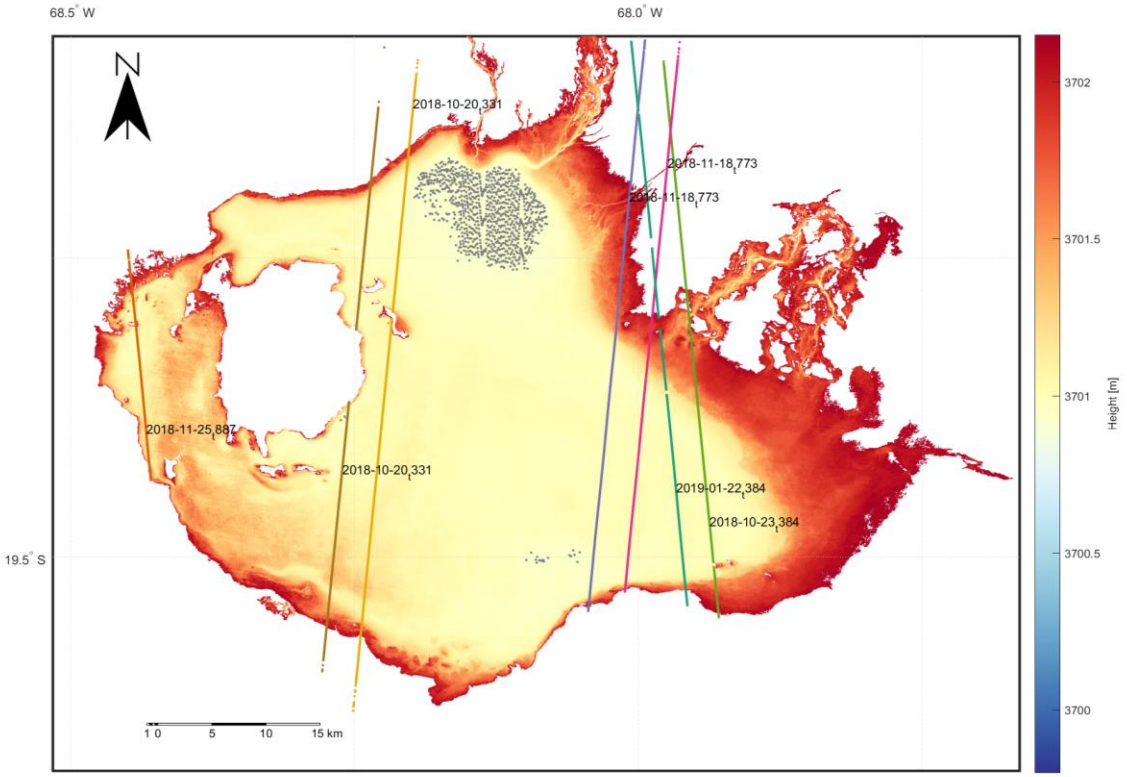

Figure S8. As in Figure S5, but for the "dry" WOLP bathymetry of Lago Coipasa.

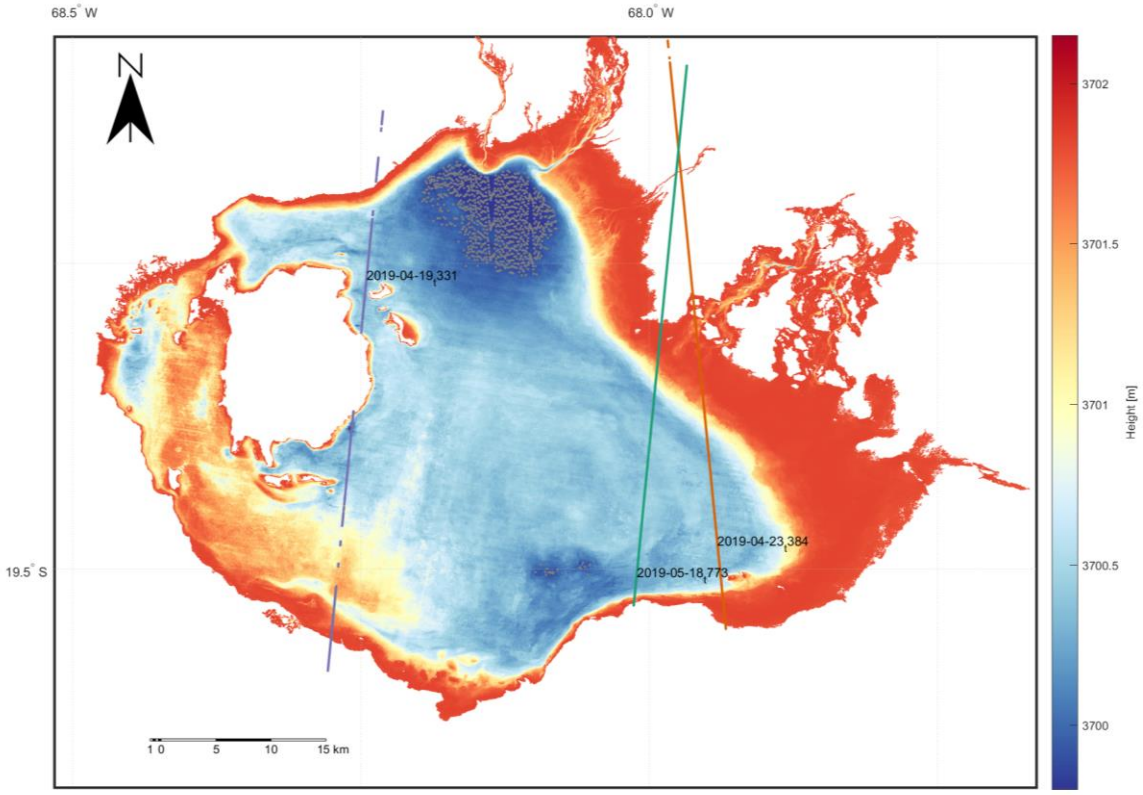

Figure S9. As in Figure S5, but for the "wet" WOLP bathymetry of Lago Coipasa.

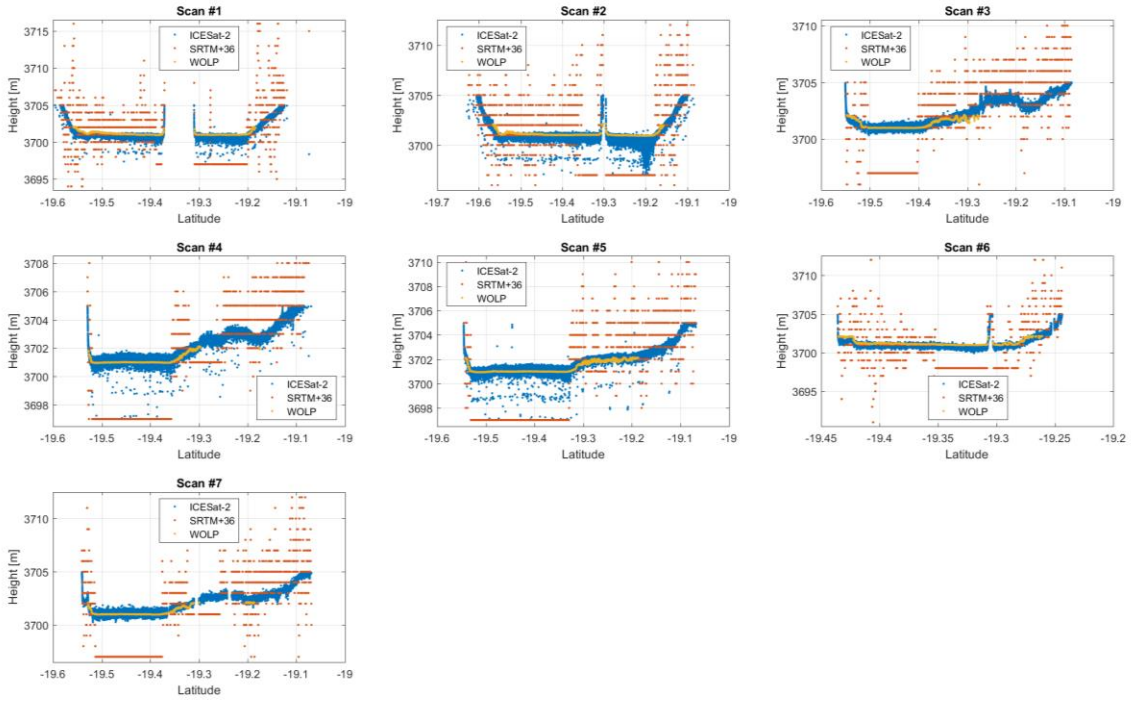

Figure S10. As in Figure S6, but for the "dry" WOLP bathymetry of Lago Coipasa.

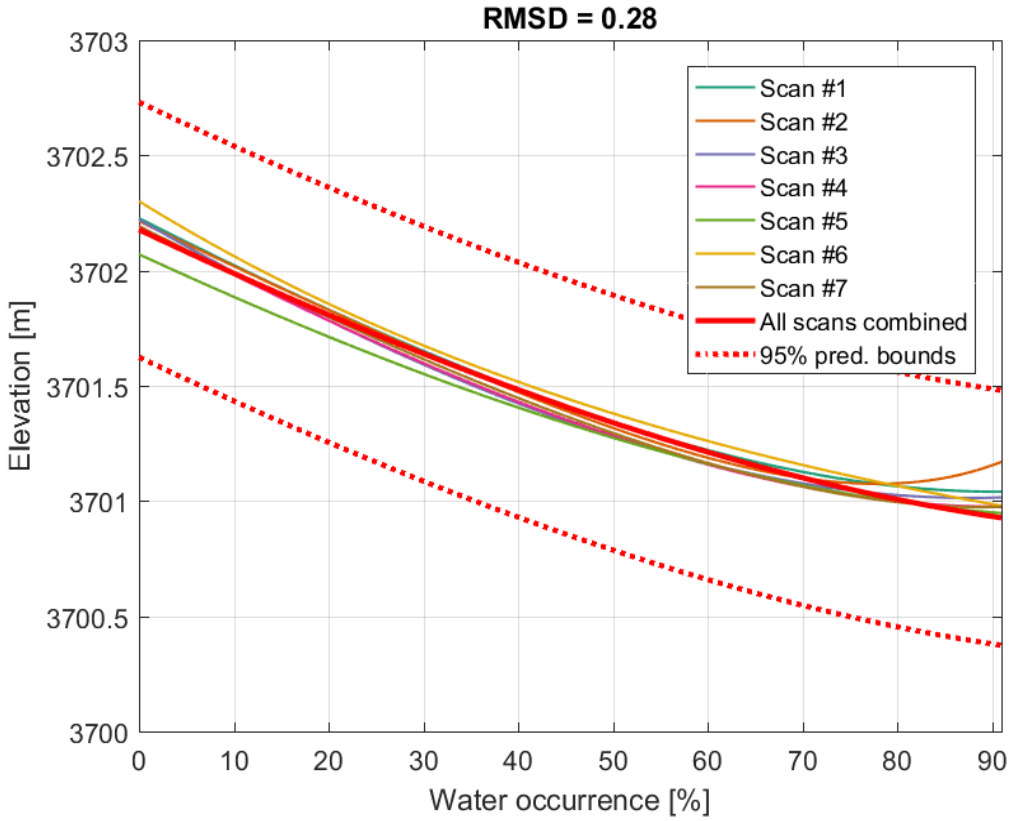

Figure S11. As in Figure S7, but for the "dry" WOLP bathymetry of Lago Coipasa. Fits were made using a 2-term exponential function.

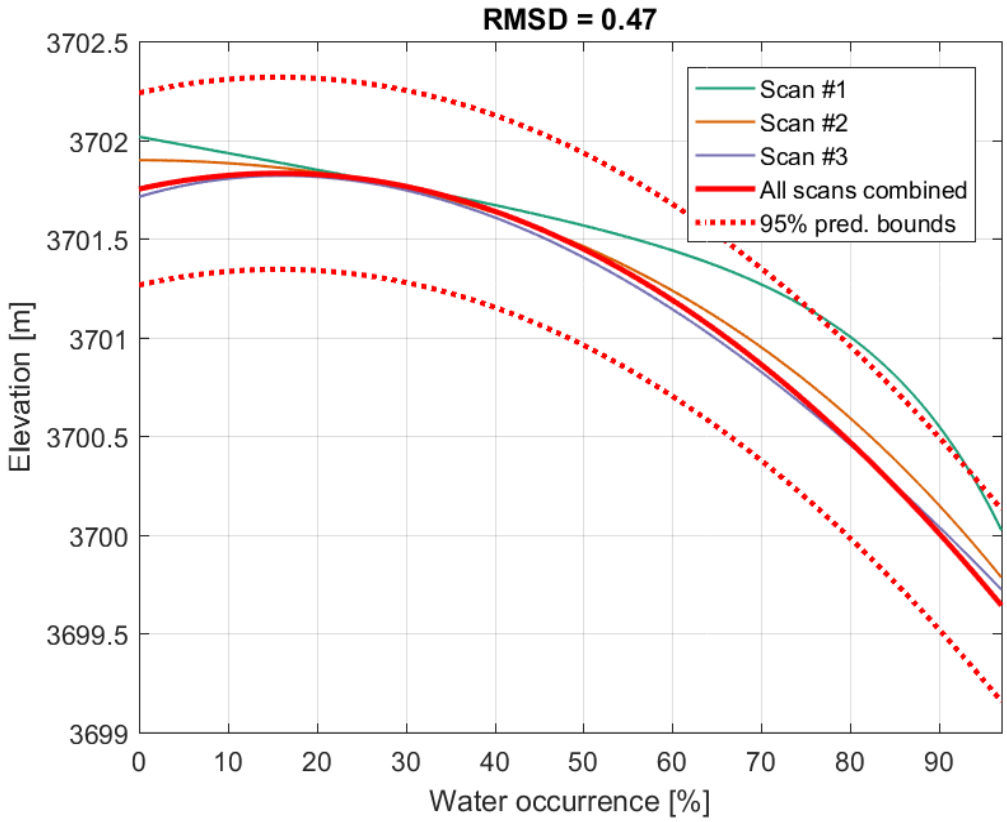

Figure S12. As in Figure S11, but for the "wet" WOLP bathymetry of Lago Coipasa.

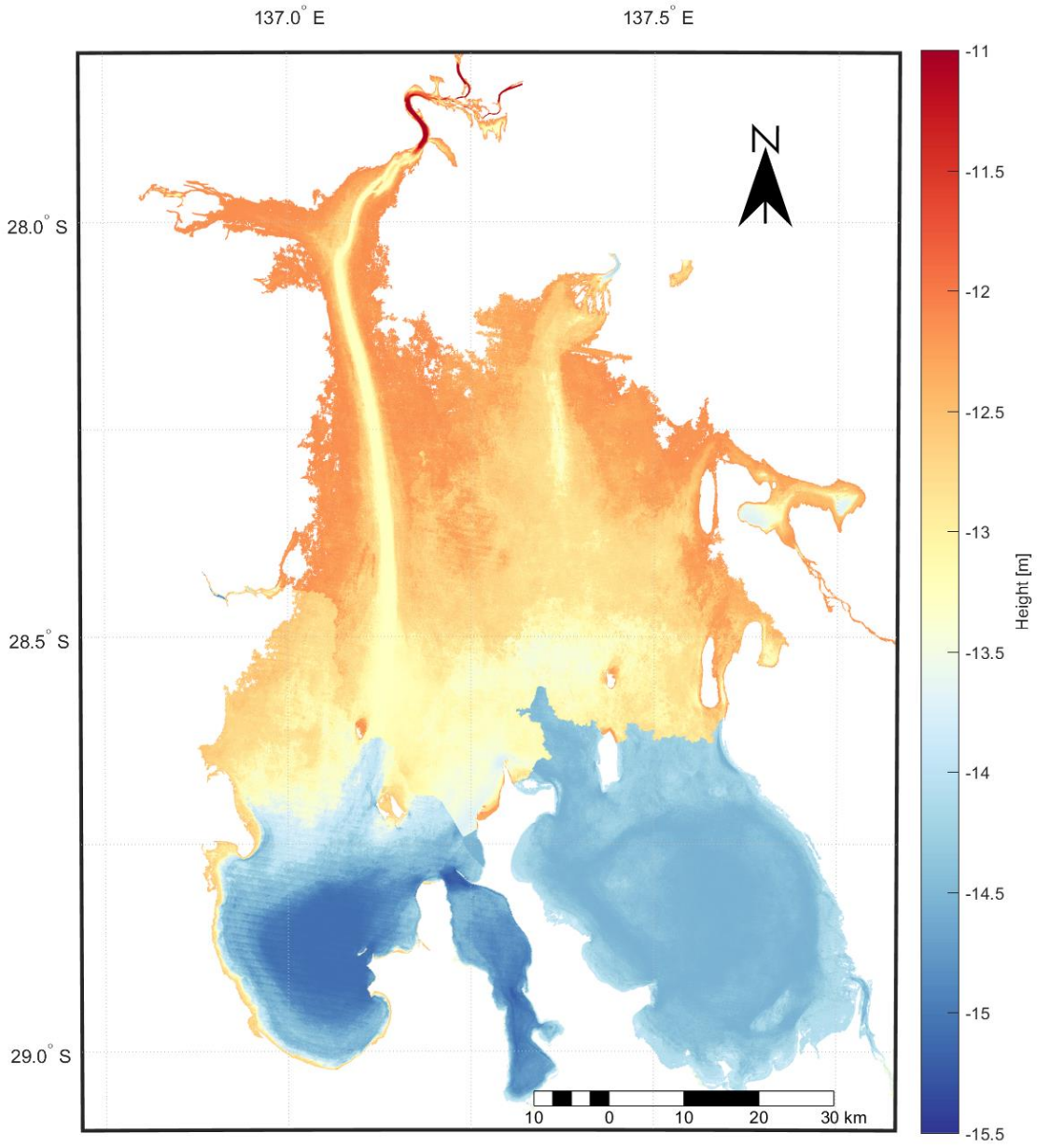

Figure S13. Step-like topography when ascribing each pixel with a single value based on the relation of water occurrence and elevation in each sub-basin. Please note the difference with respect to Figure 1d.

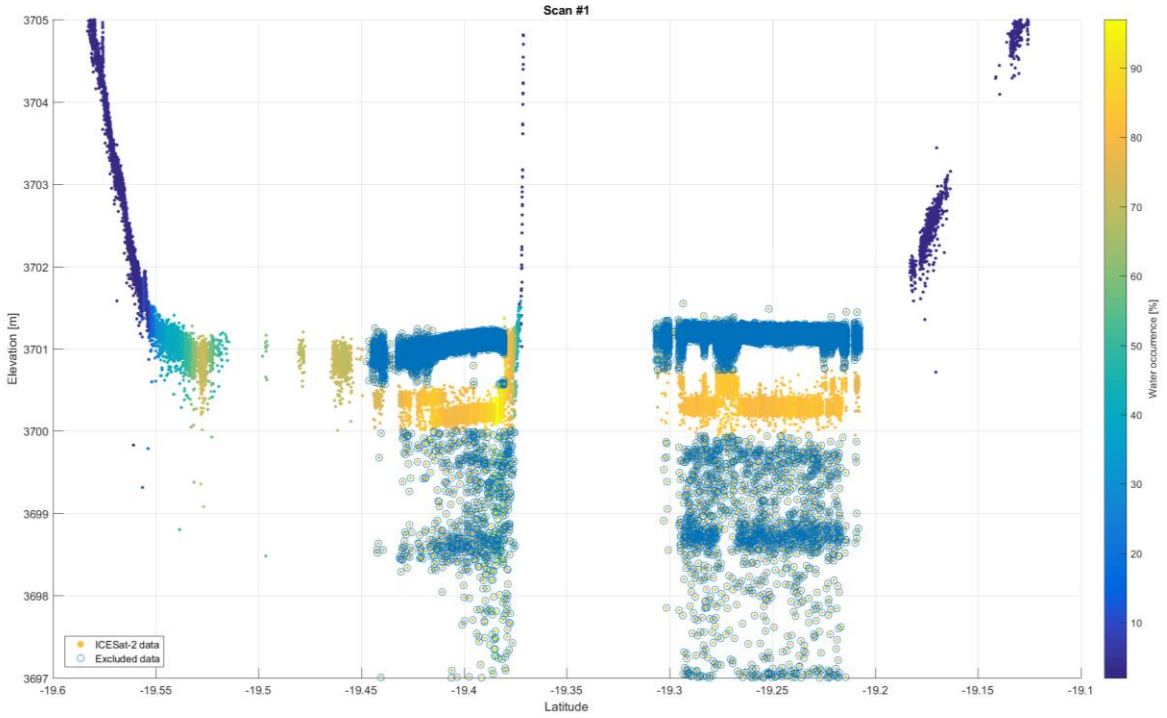

Figure S14. An example for lake-floor extraction in Lago Coipasa from "wet" scan #1 (Figure S9).

Movie S1. Time series of true-color satellite imagery of Lake Eyre showing floods that occurred between March and August 2019. Images are Copernicus Sentinel-2 data [2019], and were obtained from the Sentinel-hub website (https://apps.sentinel-hub.com/eo-browser/). Please notice the filling of the western sub-basin (Belt Bay), while the eastern sub-basin (Madigan Gulf) stays mostly dry throughout these floods.

Movie S2. Similar to Movie S1, but for the Lago Coipasa flood in February 2019.